

Missile Guidance Algorithm Against High-*g* Barrel Roll Maneuvers

Fumiaki Imado*

Mitsubishi Electric Corporation, Hyogo 661, Japan

and

Susumu Miwa†

Tokyo Denki University, Tokyo 101, Japan

The features of high-*g* barrel rolls for an aircraft and the countermeasures for a proportional navigation guidance missile against this maneuver are studied. First, the features of the barrel roll maneuver, and the effects of the parameters on the miss distance are discussed. The simulation results show that a high-*g* barrel roll maneuver generally produces a larger miss distance than a split-S (a sustained maximum *g* turn) and the miss distance does not critically depend on the maneuver initiation time, if the aircraft has a certain length of “time-to-go” and maneuvers with an appropriate roll rate. Second, the inference is made that the provision of a phase lead in the pitch-yaw plane in the missile guidance loop and adoption of the augmented proportional navigation guidance may be effective. It is also proven that a large phase shift (but less than $\pi/2$) results in a smaller miss distance and that the combination of the phase lead and the augmented proportional navigation produces better results.

Nomenclature

a_p, a_y	= missile pitch and yaw axis lateral acceleration
a_{pc}, a_{yc}	= missile pitch and yaw axis lateral acceleration commands
a_{po}, a_{yo}	= original signals (without limitation) of a_{pc} and a_{yc}
a_{po}^*, a_{yo}^*	= modified a_{po} and a_{yo} with phase lead
a_{tp}, a_{ty}	= aircraft acceleration pitch and yaw components measured in missile body axes
C_D, C_{D0}	= drag coefficient and zero-lift drag coefficient
$C_L, C_{L\alpha}$	= lift coefficient and its partial derivative of α
D	= drag
g	= acceleration of gravity
g_{bias}	= pitch bias command to compensate for gravity
h	= altitude
K	= seeker stabilization gain
K_1, K_2, K_3	= guidance loop gains
k	= induced drag coefficient of aircraft
k_1, k_2	= drag coefficients of missile
L	= lift
m	= mass
N_e	= effective navigation ratio
q	= pitch rate
RS	= random error slope
S	= Laplace operator
S_r	= aircraft reference area
T	= thrust
T_1, T_N	= seeker and noise filter time constant, respectively
v, v_c	= velocity and closing velocity
x, y	= down and cross range
α, α_c	= angle of attack and its command
α_0	= zero lift angle
γ, ψ	= aircraft flight-path and azimuth angle

δ	= missile fin angle
λ	= normalized adjoint time
ρ	= air density
σ	= line-of-sight angle
ϕ	= aircraft bank angle
ϕ_L	= missile phase shift compensation angle in pitch and yaw plane
ω	= aircraft barrel roll rate
(\cdot)	= time derivative
(\cdot)	= estimated or filtered value

Subscripts

c	= command
m, t	= missile and aircraft
p, y	= pitch and yaw
0	= initial value
max	= maximum value

Introduction

MANY studies have been performed on the optimal evasive maneuver of an aircraft against a proportional navigation missile. To obtain the optimal aircraft maneuver, a high-dimensional, nonlinear, two-point boundary value problem must be solved. Because of the difficulty inherent to this problem, most of the earlier works use very simple aircraft and missile models, and only a few deal with the three-dimensional problem.¹

The results of the earlier two-dimensional studies showed that optimal evasive maneuvers become a split-S type or a vertical-S type.^{2,3} As these maneuvers are two-dimensional in nature, the previous results are valid and may be proved to be optimum in a neighboring extremal sense. The high-*g* barrel roll (HGB) maneuver,^{4,5} which is well-known to pilots, however, cannot be analyzed by a two-dimensional study because of its essentially three-dimensional nature.^{6,7}

In the first part of this paper, the features of the HGB maneuver against a proportional navigation guidance (PNG) missile are studied. Parametric studies are conducted, although not in the optimization standpoint, by using a three-dimensional, pursuit-evasion mathematical model, and the effects of time-to-go, aircraft barrel roll rate, missile time constant, and other parameters on the miss distance are analyzed.

Received Aug. 29, 1991; revision received March 20, 1993; accepted for publication April 4, 1993. Copyright © 1993 by the American Institute of Aeronautics and Astronautics, Inc. All rights reserved.

*Chief Engineer, Mechanical Systems and Technology Department, Central Research Laboratory. Member AIAA.

†Professor, Faculty of Engineering.

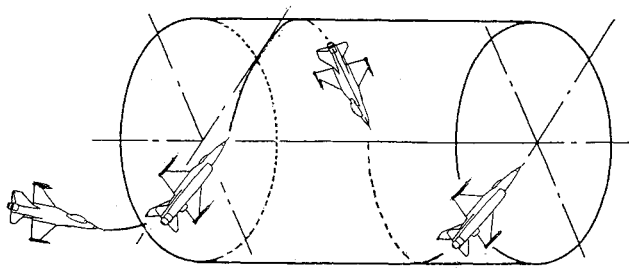
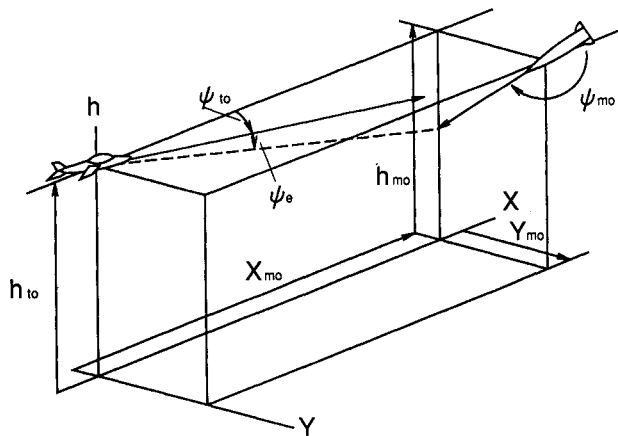
Fig. 1 Typical high-*g* barrel roll flight pattern.

Fig. 2 Geometry.

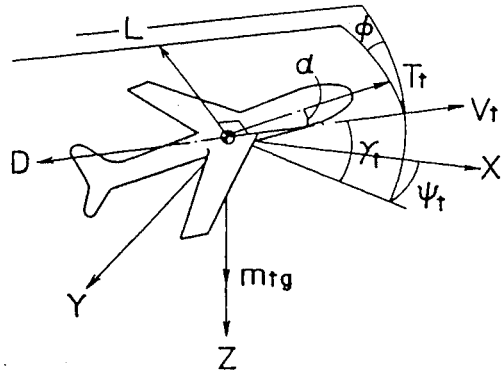


Fig. 3 Aircraft symbols.

In the second part of this paper, missile countermeasures against the HGB are discussed. Addition of a phase shift to the missile lateral acceleration command signal in the pitch-yaw plane and adoption of the augmented PNG (APNG) are proposed. These measures and the combination of both are proven to be effective in the simulation studies.

Effectiveness of High-*g* Barrel Roll

Aircraft Models

Two aircraft models that take HGB maneuvers are considered. A conceptual HGB pattern and the coordinate system are shown in Figs. 1 and 2, respectively. Model I is a simple mathematical model that takes an ideal barrel roll trajectory with lateral acceleration a_t and barrel roll rate ω . Model II is a point-mass model shown in Fig. 3 in which no side slip is assumed (i.e., the side-slip angle is always reduced to 0 deg by rudder control). This model represents an aircraft more realistically; however, it takes on a somewhat deformed barrel roll.

The equations employed for these models are as follows.

For model I:

$$\ddot{y}_t = a_t \cos \omega t \quad (1)$$

$$\ddot{z}_t = a_t \sin \omega t \quad (2)$$

with initial conditions at time $t = 0$

$$\dot{x}_{t0} = -v_t, \quad x_{t0} = \text{given} \quad (3)$$

$$\dot{y}_{t0} = 0, \quad y_{t0} = -(a_t/\omega^2) \quad (4)$$

$$\dot{z}_{t0} = -(a_t/\omega), \quad z_{t0} = 0 \quad (5)$$

The resulting trajectory is given by

$$x_t = x_{t0} - v_t t \quad (6)$$

$$y_t = -(a_t/\omega^2) \cos \omega t \quad (7)$$

$$z_t = (a_t/\omega^2) \sin \omega t \quad (8)$$

For model II:

$$\dot{v}_t = (1/m_t)(T_t \cos \alpha - D) - g \sin \gamma_t \quad (9)$$

$$\dot{\gamma}_t = (1/m_t v_t)(L + T_t \sin \alpha) \cos \phi - (g/v_t) \cos \gamma_t \quad (10)$$

$$\dot{\phi} = \frac{L + T_t \sin \alpha}{m_t v_t \cos \gamma_t} \sin \phi \quad (11)$$

$$\dot{x}_t = v_t \cos \gamma_t \cos \psi_t \quad (12)$$

$$\dot{y}_t = v_t \cos \gamma_t \sin \psi_t \quad (13)$$

$$\dot{z}_t = v_t \sin \gamma_t \quad (14)$$

where

$$L = \frac{1}{2} \rho v_t^2 s_t C_L \quad (15)$$

$$C_L = C_{L\alpha}(\alpha - \alpha_0) \quad (16)$$

$$D = \frac{1}{2} \rho v_t^2 s_t C_D \quad (17)$$

The aircraft is assumed to be controlled by thrust T_t , angle of attack α , and bank angle ϕ . The nominal values and the initial conditions are shown in Table 1. The trajectory is computed by using Eqs. (9-17).

Missile Model

A conceptual medium range air-to-air missile is considered where fairly precise missile dynamics having six degrees of freedom are provided.⁸ Figure 4 shows the pitch guidance loop, which is typical of a roll-stabilized missile,⁹ and has a rate and acceleration feedback-type autopilot. The estimated value of the target acceleration component projected to the missile ($-z$) axis, shown as \hat{a}_{tp} in the figure, is added to an APNG missile, but not to a PNG missile. The yaw guidance loop is almost the same as the pitch channel, except that the g_{bias} term is eliminated.

The nominal parameters and the initial conditions of the missile are also included in Table 1. The missile is assumed to be in the sustainer stage, and in the "head-on" geometric angle to the aircraft. The aircraft initiates a HGB maneuver a few seconds before interception.

Simulation Results

Miss distances are investigated first on a model I aircraft against a missile. Figure 5 shows the miss distance vs time-to-go (interception time minus maneuver initiation time)

Table 1 Nominal parameter

Aircraft model I:	
a_t	= 7 g (sustained)
Aircraft model II:	
m_t	= 7500 kg
s_t	= 26.0 m ²
v_{t0}	= 290 m/s
h_{t0}	= 3000 m
x_{t0}	= 0 m
Ψ_{t0}	= 0 deg
$C_{L\alpha}$	= 4.01 /rad
C_{D0}	= 0.0169
k	= 0.179
T_t	= 65,000 N
Missile:	
m_{m0}	= 176 kg
T_{m0}	= 5880 N
v_{m0}	= 720 m/s
h_{m0}	= 3000 m/s
x_{m0}	= 5000 m
Ψ_{m0}	= 180 deg
RS	= 0 deg/deg
T_1	= 0.10 s
T_N	= 0.11 s
N_e	= 4
K_{SL}	= 200
K_1 ,	= 4.0 /s
K_2 ,	= 0.1 s
K_3 ,	= 0.1 s/m
a_{pcmax}	= 30 g
a_{ycmax}	= 30 g

for various aircraft HGB roll rates. With more than 2 s of time-to-go left at $\omega = 1-3$ rad/s, a fairly large miss distance is always obtained. The maximum miss distance occurs at $\omega = 1.5-2$ rad/s. For $\omega > 2$ rad/s, the barrel roll radius becomes less than 17 m, which results in smaller miss distances.

This model has the merit of taking a complete barrel roll but has a couple of disadvantages. One is that the miss distance takes a high value for short time-to-go of less than 1 s because the target has an initial lateral velocity; the other is that the target velocity becomes so large for the small value of ω that an unreasonably large miss distance occurs in these cases. The $\omega = 0$ and 0.5 rad/s cases are thus eliminated from the figure.

Miss distances are also checked using aircraft model II, which is closer to the actual aircraft. The α_c value of 0.129 rad is determined to give the aircraft lateral acceleration of about 7 g. The aircraft thrust is not taken from the actual data, but rather to maintain a corner speed of about 290 m/s. Unfortunately, the aircraft is unable to stay on the barrel for the higher roll rate because its maximum load factor is limited. However, this model does not show the defects of model I.

Figure 6 shows the time-to-go vs miss distance for various ω , which corresponds to Fig. 5 of model I. The tendencies are the same for longer time-to-go and higher ω values. The miss distance becomes large and irrelevant to a time-to-go of larger than 3 s if the roll rate is 1-3 rad/s. On the other hand, in the case of $\omega = 0$, which corresponds to a split-S in the two-dimensional maneuver, or in $\omega = 0.5$ rad/s, the miss is relatively small and critically depends on the time-to-go value. In other words, the evasive maneuver has to be started about 1 s before interception in these cases. From these analyses, it can be said that the HGB is effective if the aircraft takes the maneuver earlier with the proper roll rate.

Figure 7 shows how the miss distance of the model II aircraft changes with respect to the missile noise filter time constant. Generally, the miss distance becomes smaller for the small missile time constant in the noise-free system. This tendency is apparent from the figure. Figure 8 depicts the effect of the missile proportional navigation constant, where the miss distances are calculated for a time-to-go value of 6 s using the model II aircraft. The ω value corresponding to the peak miss becomes greater as N_e increases.

Trajectory Analysis

Trajectory analyses were conducted to clarify the nature of the HGB maneuver. Figure 9 shows one of the analytical and numerical study results of the missile trajectories in the $y - z$ plane together with that of the model I aircraft. A simpler missile model with the initial velocity to the z direction is used in this study.⁶ This figure shows the $\omega = 1$ rad/s case, and λ in the figure is a normalized adjoint time: $\lambda = 1$ and 0 indicate the initial and final positions of the vehicles, respectively. It is seen that the missile cannot follow the aircraft at the initial stage and goes far away in the z direction. These trajectories provided us with the insight that the HGB may defeat the PNG-type missile from the control system point of view, and that it is necessary to consider the new missile guidance algorithm in this study.

Missile Guidance Algorithm

Concept

So far the characteristics of the HGB have been clarified. The next step is to find the countermeasure against this ma-

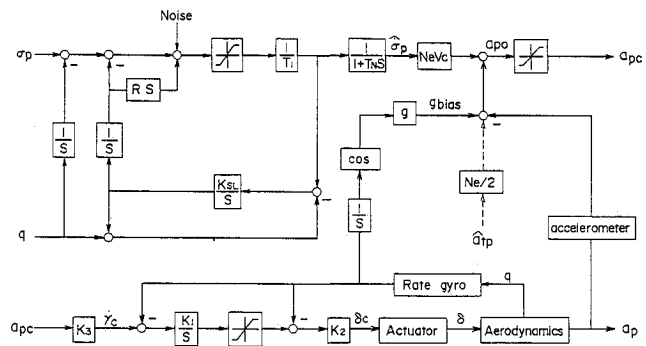


Fig. 4 Missile pitch guidance loop.

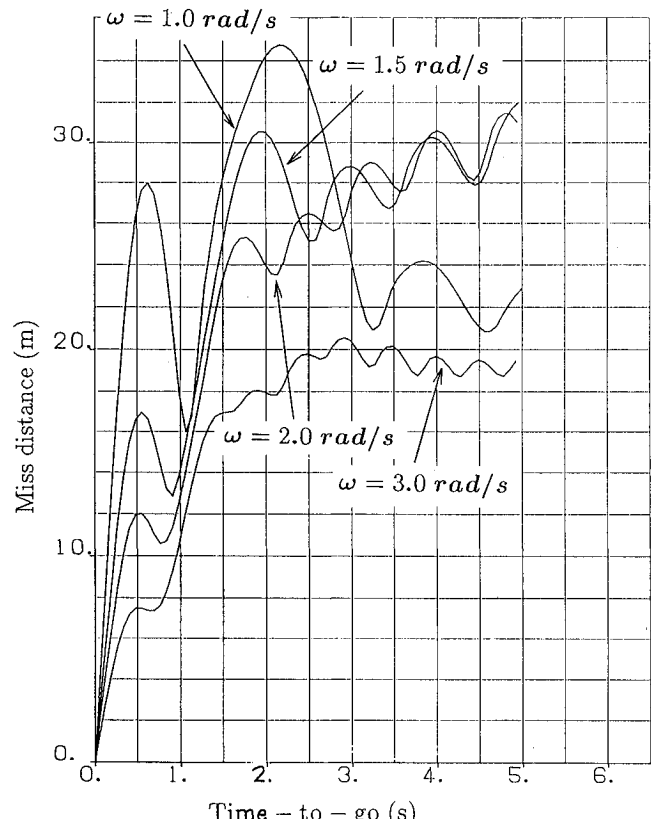


Fig. 5 Effect of time-to-go and roll rate for model I.

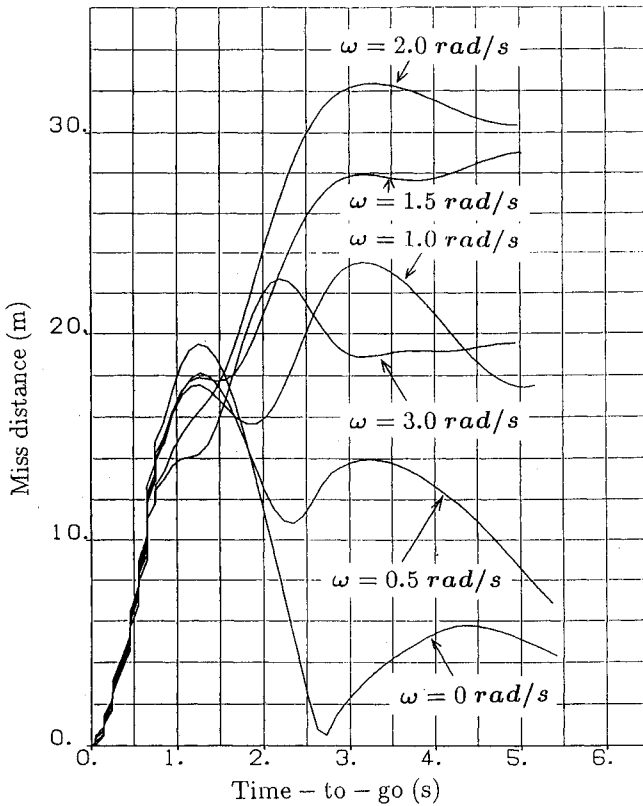


Fig. 6 Effect of time-to-go and roll rate for model II.

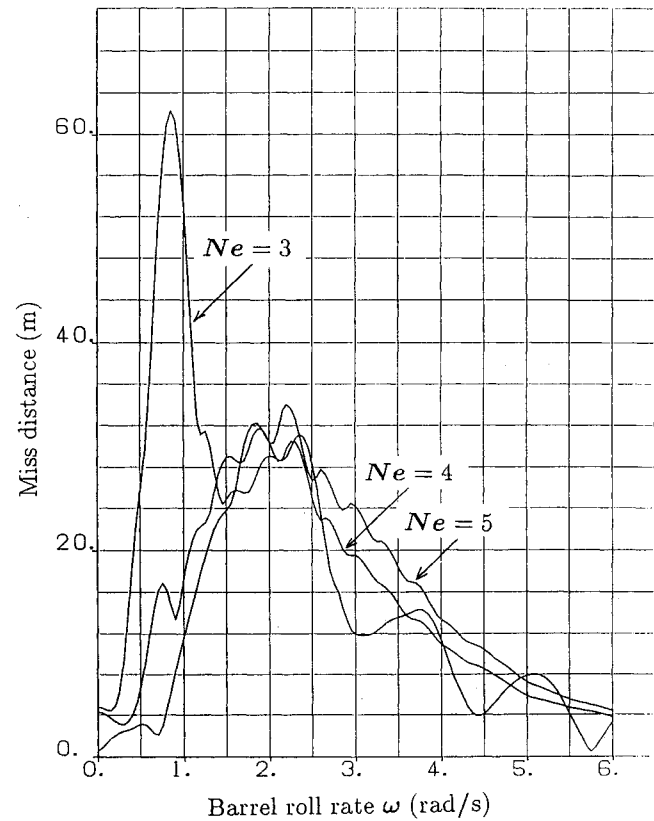


Fig. 8 Effect of navigation constant.

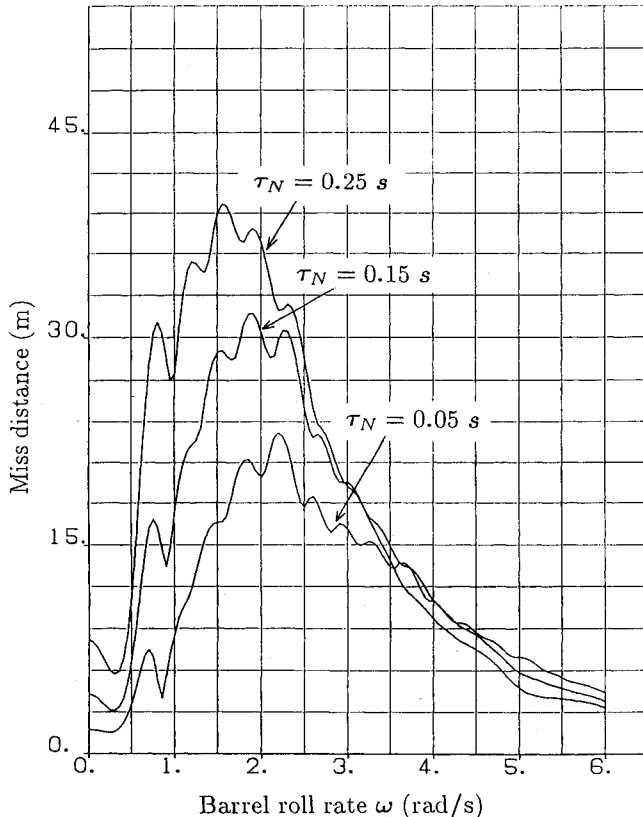


Fig. 7 Effect of time constant.

neuver. The aircraft's two-dimensional evasive maneuvers, such as the split-S (a kind of sustained maximum g turn) or the vertical-S, make use of the transient response of a missile guidance loop, whereas the HGB seems to utilize the coupling between the pitch and yaw channels. Maneuvering an aircraft with HGB is observed as a successive change of line-of-sight (LOS) rate for a missile seeker. It is therefore conceivable that rotating the missile's lateral acceleration command signal in the pitch-yaw plane will help to reduce the miss distance. This may also reduce the excessive swing of the missile trajectory shown in Fig. 9.

From a different point of view, the circular aircraft movement in the y - z plane constantly generates a centripetal acceleration. Therefore, the APNG, which compensates for the target acceleration, seems to be effective against the HGB.

Missile Model Modification

To introduce the phase lead ϕ_L in the missile's pitch-yaw guidance channel, a_{po}^* and a_{yo}^* shown hereafter, are introduced in place of a_{po} in Fig. 4 and its corresponding signal a_{yo} in the yaw channel.

$$a_{po}^* = (a_{po} - g_{bias})\cos \phi_L + a_{yo}\sin \phi_L + g_{bias} \quad (18)$$

$$a_{yo}^* = (-a_{po} + g_{bias})\sin \phi_L + a_{yo}\cos \phi_L \quad (19)$$

If the APNG is needed, the term \hat{a}_{tp} and \hat{a}_{ty} has to be added as shown with dotted lines in Fig. 4.

Effect of Phase Shift

Various phase leads were applied to a PNG and an APNG missile, and simulation studies are conducted. First, the model I aircraft is used against the PNG missiles. Figure 10 shows the time-to-go vs miss distance for various values of the ϕ_L in the $\omega = 2$ rad/s case. The $\phi_L = 0$ rad case in the figure corresponds to the $\omega = 2$ rad/s case in Fig. 5.

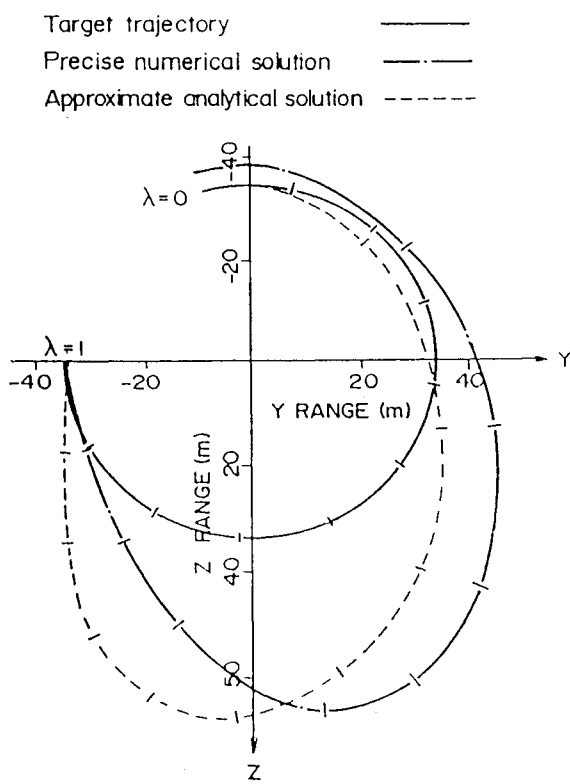


Fig. 9 Example of vehicle trajectories.

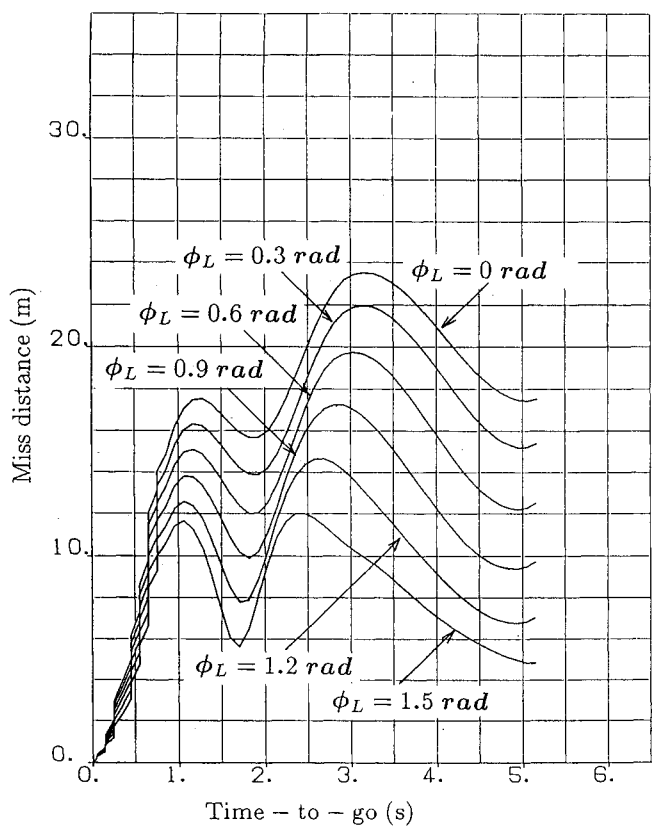


Fig. 11 Effect of phase shift (model II, 1 rad/s).

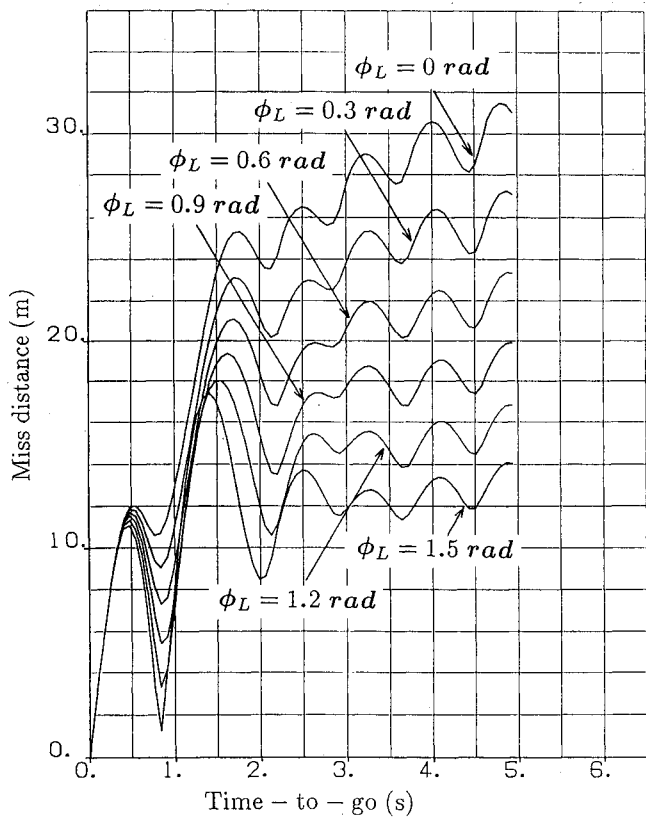


Fig. 10 Effect of phase shift (model I, 2 rad/s).

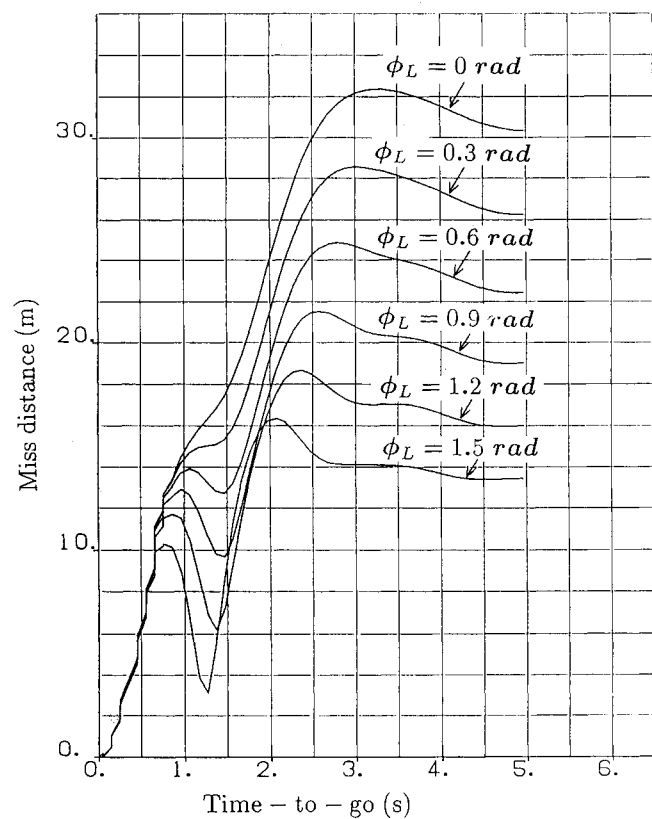


Fig. 12 Effect of phase shift (model II, 2 rad/s).

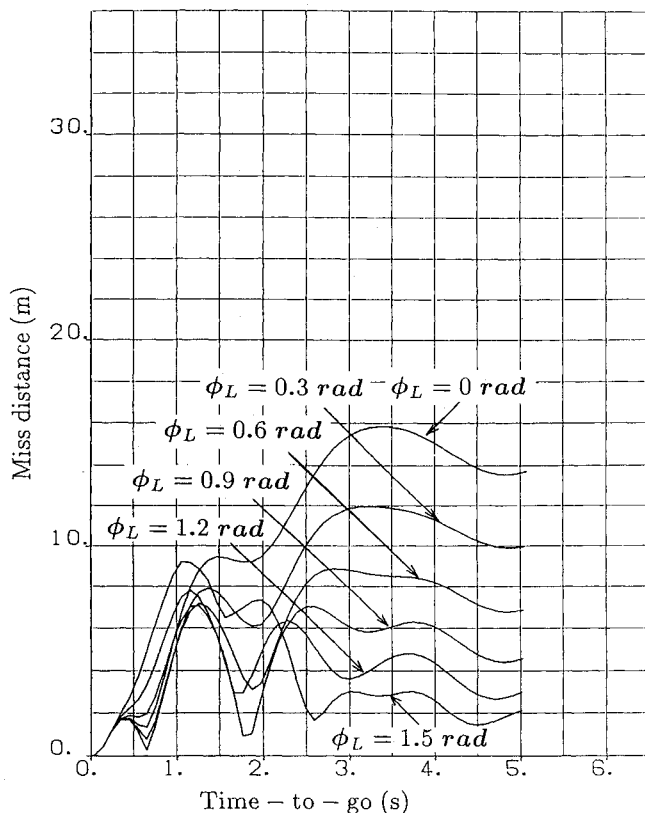


Fig. 13 Effect of phase shift plus augmented proportional navigation.

It was first expected that the optimal ϕ_L value may be found to correspond to different ω values. The result shows, however, that the miss distance monotonously decreases as ϕ_L increases from 0 to 1.5 rad. The miss distance of about 30 m in the without phase lead case goes down to approximately 13 m in the $\phi_L = 1.5$ rad case. A ϕ_L value larger than $\pi/2$ was not adopted because this brings about (although not always) guidance instability. Although not shown in the figures, negative values of ϕ_L yield the larger miss distances, a phenomenon which is reasonably understood.

Figures 11 and 12 show the results where the model II aircraft was used against the PNG missile. Figure 11 shows the case of $\omega = 1$ and Fig. 12 is for $\omega = 2$ rad/s. Again, the $\phi_L = 0$ rad case in these figures is the same as the $\omega = 1$ and 2 rad/s cases in Fig. 6. It is seen that the tendencies are the same even in the more realistic model. The miss distance of about 30 m in the without phase lead case of Fig. 12 reduces to approximately 14 m in the $\phi_L = 1.5$ rad case. Through these figures, it is found that the phase lead is always effective, and with $\phi_L = 1.5$ rad, the miss distance reduces to about the half compared with the $\phi_L = 0$ rad (without phase lead) case.

In Fig. 13, the model II aircraft and the APNG missile are used in the simulation. It shows that the APNG itself can reduce the miss distance, and that the phase lead effect is more remarkable when applied to the APNG. With more than $\phi_L = 1.2$ rad for the time-to-go of more than 3 s, the miss reduces to a few meters from the 30 m of the original case.

To implement the APNG, the target acceleration pitch and yaw components a_{tp} and a_{ty} must be estimated. This may not be an easy task, but in principle these estimated components \hat{a}_{tp} and \hat{a}_{ty} may be obtained from σ_p and σ_y by employing a

Kalman filter. The HGB maneuver of a target may also be detected by examining the amplitudes of \hat{a}_{tp} and \hat{a}_{ty} , and the roll rate can be estimated. Once estimated, the acceleration command signals are transformed by the ϕ_L operators, which are Eqs. (18) and (19). A negative ϕ_L must be employed if with a negative roll rate.¹⁰

Conclusions

The characteristics of the high- g barrel roll, a typical aircraft evasive maneuver, against a proportional navigation missile was studied first. A simplified aircraft model that performs an ideal barrel roll was used and parameter studies were conducted. The results show that the high- g barrel roll generally produces a large miss distance and that the miss distance does not critically depend on the maneuver initiation time if the aircraft has a roll rate of 1 ~ 2 rad/s and has a time-to-go of more than 3 s. This was also verified by using a point-mass aircraft model, which was more realistic but gave a somewhat deformed barrel roll trajectory; it was also made clear that the miss distance produced by the barrel roll is larger than that produced by the split-S. Other facts revealed are that the barrel roll rate, which gives a maximum miss distance, increases as the miss distance constant increases and as the missile time constant decreases.

The missile trajectory pursuing an aircraft executing a barrel roll suggested the introduction of a phase shift to the missile pitch-yaw command signal. The simulation results indicated that as the phase shift angle increases from 0 to 1.5 rad, the miss distance decreases monotonously, and that this trend does not change with variation of the roll rate or with the aircraft model. The introduction of the phase shift increases the effectiveness of the augmented proportional navigation missile. The miss distance reduces to approximately one-half for the proportional navigation and even less for the augmented navigation.

Acknowledgment

The authors are indebted to S. Uehara, Director General for Research and Development of the Japan Defence Agency, for giving us useful advice and discussing the paper.

References

- 1Shinar, J., Rotzstein, Y., and Bezner, E., "Analysis of Three-Dimensional Optimal Evasion with Linearized Kinematics," *Journal of Guidance and Control*, Vol. 1, No. 5, 1979, pp. 353-360.
- 2Forte, I., Steinberg, A., and Shinar, J., "The Effects of Non-Linear Kinematics in Optimal Evasion," *Optimal Control Applications and Methods*, Vol. 4, 1983, pp. 139-152.
- 3Imado, F., and Miwa, S., "Fighter Evasive Maneuvers Against Proportional Navigation Missile," *Journal of Aircraft*, Vol. 23, No. 11, 1986, pp. 825-830.
- 4Zarchan, P., "Representation of Realistic Evasive Maneuvers by the Use of Shaping Filters," *Journal of Guidance and Control*, Vol. 2, No. 4, 1979, pp. 290-295.
- 5Gunston, B., and Spick, M., *Modern Air Combat*, Salamander Books Ltd., London, 1983, p. 202.
- 6Imado, F., and Miwa, S., "Three-Dimensional Study of Evasive Maneuvers of a Fighter Against Missiles," AIAA Paper 86-2038-CP, 1986.
- 7Imado, F., and Miwa, S., "Fighter Evasive Boundaries Against Missiles," *Computers Mathematics with Applications*, Vol. 18, No. 1-3, 1989, pp. 1-14.
- 8Garnell, P., *Guided Weapon Control Systems*, 2nd ed., Pergamon Press, Oxford, England, UK, 1980.
- 9Nesline, F. W., and Zarchan, P., "Missile Guidance Design Trade-Offs for High-Altitude Air Defense," *Journal of Guidance and Control*, Vol. 4, No. 5, 1981, pp. 207-212.
- 10Imado, F., and Miwa, S., "An Efficient Guidance Algorithm Against High- g Barrel Roll Maneuvers," AIAA Paper 90-3342-CP, 1990.